

# PHY 982 Homework 2

John Ash, Mengzhi Chen, Tong Li, Jason Surbrook

February 27, 2018

## 1 Elastic scattering calculations between nucleons and $^{208}\text{Pb}$ target

### 1.1 Coulomb scattering

In the case of point-Coulomb scattering, the Coulomb interaction between the projectile and the target with charges  $Z_1$  and  $Z_2$  is

$$V_c(R) = \frac{Z_1 Z_2 e^2}{R^2}, \quad (1)$$

where  $R$  is the distance between them. The Schrödinger's equation with this potential can be solved analytically. Related discussions are detailed in Ref.[1]. In sum, the angular distribution of point-Coulomb potential is described by the differential cross section

$$\sigma(\theta) = \frac{\eta^2}{4k^2 \sin^4(\theta/2)}; \quad \eta = \frac{Z_1 Z_2 e^2}{\hbar} \left( \frac{\mu}{2E} \right)^{\frac{1}{2}}, \quad (2)$$

where  $\mu$  is the reduced mass and  $k$  is the wave number with the energy  $E$ . It worth noticing that the Eq. 3 is the same as the classical *Rutherford cross section*.

When the finite size of the target is included, due to different charge distributions, the interaction between the projectile and the target becomes more complicated. The case for uniform distribution over a sphere are formulated in Ref. [1].

Normally, these potentials are not analytically solvable. Sometimes, we can apply the *plane wave Born approximation* (PWBA) for the Coulomb scattering. Under PWBA, the differential cross section is

$$\sigma(\theta) = \frac{\eta^2}{4k^2 \sin^4(\theta/2)} |F(\theta)|^2, \quad (3)$$

where  $F(\theta)$  is called the *form factor* related with the charge distribution as

$$F(\theta) = \int e^{i(\vec{k}_f - \vec{k}_i) \cdot \vec{r}'} \rho(r') d^3 r'. \quad (4)$$

In sum, we see the finite size of the target can give cross sections different from the point-like case.

## 1.2 The optical potential

In this section, we study the elastic scattering between nucleons and the  $^{208}\text{Pb}$  target with the help of FRESKO[2]. Their effective interaction is referred to as the optical potential. We take the global parameterization from Ref. [3, 4] as the input for FRESKO.

In the first step, we take two lab energies 5 and 50 MeV in our calculation. The results are shown in Figure 1. It gives the angular distributions in center of mass for protons and neutrons. For the 5 MeV proton, the curve agrees well with the *Rutherford cross section*. Given that the radius parameter of optical potential is  $r_w \sim 1.2 \text{ fm}$ , we can estimate the Coulomb barrier for a proton to overcome. It should be

$$E_{Coul} \approx \frac{Z_1 Z_2 e^2}{r_w + R_2} \approx 15 \text{ MeV}. \quad (5)$$

We see that 5 MeV is much lower than the Coulomb barrier. Thus, this scattering can be referred as a point-like Coulomb scattering properly. The agreement with the *Rutherford cross section* also verifies this point. For neutrons, there is no Rutherford scattering cross section to compare against, hence the value of the neutron cross section being listed as  $\text{fm}^2$ . At 5 MeV the cross section hints at a broad diffraction pattern. Since 50 MeV is strong enough to overcome the Coulomb barrier, the effective interaction plays a role and induces a diffraction pattern in Figure 1. The neutron cross section exhibits a similar behavior, speaking to the dominance of the nuclear interaction at this energy. In order to explore the influence of the optical potential, we will use  $E_{lab} = 50 \text{ MeV}$  in our following calculations.

In our next step, we would like to see the influences of the depth of optical potential's imaginary part of the S-matrix. Fixing other parameters, we scale the depth of imaginary parts  $V_i$  (including volume, surface derivative and spin-orbit potentials) a factor of 1.5, 0.5 and 0. The modules of S-matrix with for the proton and the neutron are shown in Table 1 and 2. We can see that as we lower the depth,  $|\mathbf{S}|^2$  fluctuates and eventually converges to one which indicates an elastic scattering. It inspires us that the imaginary parts can describe absorptions in scattering processes. It also worth noticing the fluctuation of  $|\mathbf{S}|^2$  with varying  $V_i$  in each partial wave. For this reason, there is no simple monotonous relations between the relative depth  $\bar{V}$  and the total absorptive cross section.

Moreover, we are interested in the effects of different radius parameters. Again, fixing other parameters, we repeat our calculations by scaling the radius parameters  $r$  (including volume, surface derivative and spin-orbit potentials) a factor of 0.2, 0.5, 2, 3 and 4. The results are shown in Figure 2. For the proton, we observe the dramatic up-down shifts and denser diffraction patterns with increasing  $r$ . It's the synergistic effect by the Coulomb

Proton partial waves					
L	J	$ \mathbf{S} ^2(\bar{V}=1.5)$	$ \mathbf{S} ^2(\bar{V}=1.0)$	$ \mathbf{S} ^2(\bar{V}=0.5)$	$ \mathbf{S} ^2(\bar{V}=0.0)$
0	0.5	6.45E-04	2.33E-04	1.56E-02	1.0
1	0.5	9.17E-04	1.17E-03	1.63E-02	1.0
2	1.5	8.33E-04	1.28E-04	1.34E-02	1.0
1	1.5	9.19E-04	1.23E-03	1.74E-02	1.0
2	2.5	7.97E-04	1.17E-04	1.52E-02	1.0
3	2.5	1.27E-03	1.64E-03	1.81E-02	1.0
4	3.5	1.51E-03	2.89E-04	1.02E-02	1.0
3	3.5	1.27E-03	1.85E-03	2.11E-02	1.0
...	...	...	...	...	...

Table 1: The modules of S-matrix for proton partial waves with varying imaginary potentials, where  $\bar{V}$  is the scaled depth defined as  $V_i(new)/V_i(initial)$ .

Neutron partial waves					
L	J	$ \mathbf{S} ^2(\bar{V}=1.5)$	$ \mathbf{S} ^2(\bar{V}=1.0)$	$ \mathbf{S} ^2(\bar{V}=0.5)$	$ \mathbf{S} ^2(\bar{V}=0.0)$
0	0.5	7.96E-05	1.06E-03	8.21E-03	1.0
1	0.5	1.60E-04	2.51E-04	5.50E-03	1.0
2	1.5	1.09E-04	1.08E-03	6.26E-03	1.0
1	1.5	1.69E-04	3.06E-04	6.80E-03	1.0
2	2.5	1.16E-04	1.25E-03	8.02E-03	1.0
3	2.5	1.26E-04	1.50E-04	5.48E-03	1.0
4	3.5	1.95E-04	1.14E-03	2.21E-03	1.0
3	3.5	1.42E-04	2.61E-04	8.83E-03	1.0
...	...	...	...	...	...

Table 2: The modules of S-matrix for neutron partial waves with varying imaginary potentials, where  $\bar{V}$  is the scaled depth defined as  $V_i(new)/V_i(initial)$ .

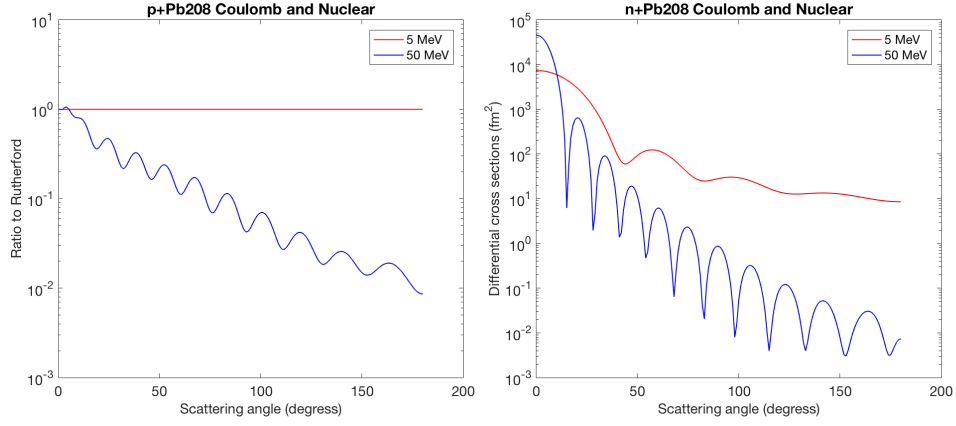


Figure 1: Differential cross sections for nucleons scattering with  $^{208}\text{Pb}$  at 5 and 50 MeV. Left panel is proton and right panel is neutron

and optical potentials. As for neutron, the changing of pattern is relative small as it only feels the optical potential.

The total reaction cross section is directly accessible in FRESKO. In order to align with existing experimental information on  $n + ^{208}\text{Pb}$ , a lab energy of 40 MeV is used. The value for this reaction's absorption cross section is 55.2 barns. Since it's a elastic scattering, the total reaction cross section takes the same value.

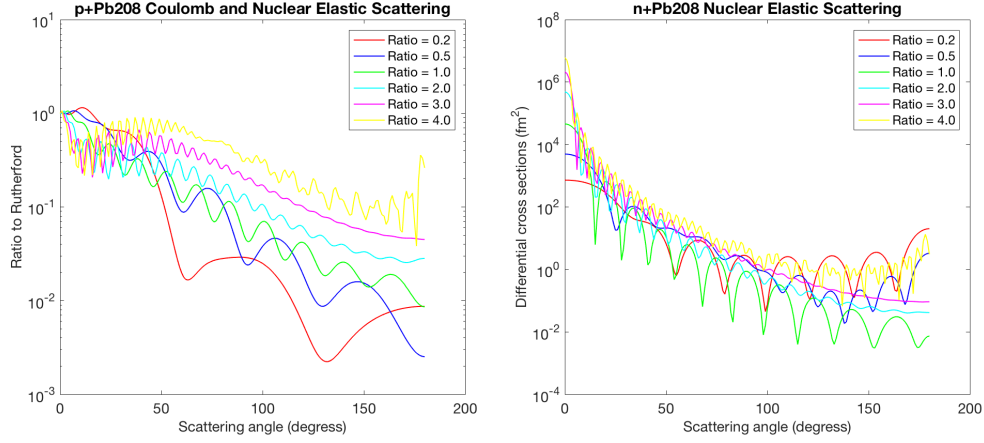


Figure 2: Differential cross sections for nucleons scattering with  $^{208}\text{Pb}$  with different radius parameters at 50MeV, where ratio is defined as  $r_{\text{new}}/r_{\text{initial}}$ . Left panel is proton and right panel is neutron

## References

- [1] Ian J Thompson and Filomena M Nunes. Nuclear reactions for astrophysics: principles, calculation and applications of low-energy reactions. pages 62–64,129–131, 2009.
- [2] I.J. Thompson. Fresco, coupled reaction channels calculations. <http://www.fresco.org.uk/>. Accessed Feb 25, 2018.
- [3] Roberto Capote, Michel Herman, P Obložinský, PG Young, Stéphane Goriely, T Belgaya, AV Ignatyuk, Arjan J Koning, Stéphane Hilaire, Vladimir A Plujko, et al. Ripl—reference input parameter library for calculation of nuclear reactions and nuclear data evaluations. *Nuclear Data Sheets*, 110(12):3107–3214, 2009.
- [4] AJ Koning and JP Delaroche. Local and global nucleon optical models from 1 kev to 200 mev. *Nuclear Physics A*, 713(3-4):231–310, 2003.